Electrochemical and Spectroelectrochemical Behavior of Cobalt(III), Cobalt(II), and Cobalt(I) Complexes of *meso*-Tetraphenylporphyrinate Bearing Bromides on the β-Pyrrole Positions

Francis D'Souza,† Anne Villard,† Eric Van Caemelbecke,† Michelle Franzen,† Tristano Boschi,‡ Pietro Tagliatesta,‡ and Karl M. Kadish*,†

Department of Chemistry, University of Houston, Houston, Texas 77204-5641, and Dipartimento di Scienze e Tecnologie Chimiche, Il Universitá degli Studi di Roma, 00173 Roma, Italy

Received February 26, 1993

The synthesis and characterization of (*meso*-tetraphenylporphyrinato)cobalt(II) complexes containing six, seven, or eight Br groups at the β-pyrrole positions of the macrocycle is reported. Each compound undergoes three one-electron oxidations and up to nine one-electron reductions depending upon the degree of Br substitution. The first oxidation yields $[(TPPBr_x)Co^{III}]^+$ while the first reduction gives $[(TPPBr_x)Co^{I}]^-$ where $TPPBr_x$ is the dianion of the brominated tetraphenylporphyrin. Cyclic voltammetry studies reveal a positive shift of the metal and ring-centered redox potentials of the bromo porphyrins as compared to $E_{1/2}$ for the reduction and oxidation of unsubstituted (TPP)Co. The optical absorption spectra of each electrogenerated Co(I) and Co(III) complex were recorded in a thin-layer cell and show that the transition energies for both the Soret and visible bands vary as a function of Br groups on the porphyrin periphery. The electron withdrawing Br substituents also produce a red shift in the Soret and visible bands of the porphyrin which follows the order: $(TPPBr_8)Co > (TPPBr_7)Co > (TPPBr_6)Co > (TPP)Co$. The singly oxidized and singly reduced products are stable on the cyclic voltammetric and thin-layer time scales, but further reductions beyond $[(TPPBr_x)Co^{I}]^-$ lead to the stepwise elimination of Br groups to give $[(TPP)Co^{I}]^-$ as a final product in solution. Results obtained by controlled-potential thin-layer spectroelectrochemistry and rotating ring disk electrode voltammetry confirm this experimental observation.

Introduction

The use of metalloporphyrins as catalysts in the oxidation of organic substrates is well documented in the literature.[1-5] A variety of porphyrin derivatives have been utilized, among which are synthetic perhalogenated tetraphenylporphyrins which show an exceptionally high catalytic efficiency.[6-24] The electron-withdrawing ability of the halogen substituents on the porphyrin periphery can activate a high-valent metal intermediate and lower the energy of the highest occupied molecular orbital (HOMO), resulting in decreased oxidative degradation reactions of the porphyrin macrocycle.[6,23,25-27]

Two main types of halogenated porphyrins have been utilized as catalysts; these are porphyrins having substituents on the β-pyrrole position[6] and those bearing substituents on the four phenyl rings of a tetraphenylporphyrin.[11,14] Recently, tetraphenylporphyrins bearing halogen substituents on both the β-pyrrole and the ortho positions of the four phenyl rings were also synthesized, and these compounds show enhanced catalytic activity.[8,11,16,20,24]

The ability of a given porphyrin to serve as an oxidation catalyst is related to its oxidation potential in the absence of a substrate. The addition of electron withdrawing groups to either the porphyrin periphery or to the four phenyl rings of a tetraphenylporphyrin will lead to a more facile reduction and a harder oxidation, with the largest effect on redox potentials being for β-substituted porphyrins which are in direct conjugation with the macrocyclic π ring system.[28] Also, the shift of $E_{1/2}$ will often vary directly with the number of electron donating or electron withdrawing substituents on the complex,[28] but this is not always the case, especially for oxidation. For example, nonlinear correlations have been reported between oxidation potentials and the number of bromo groups on the β-pyrrole positions of Cu and free base tetraphenylporphyrins containing between one and four bromo substituents,[29,30] and this was attributed to steric factors associated with the added substituents.

† University of Houston.
‡ Universitá degli Studi di Roma.

(1) McMurry, T. J.; Groves, J. T. In *Cytochrome P-450: Structure, Mechanism and Biochemistry*; Ortiz de Montellano, P., Ed.; Plenum Press: New York, 1986; Chapter 1.
(2) Bruice, T. C. In *Mechanistic Principles of Enzyme Activity*; Liberman, J. F., Greenberg, A., Eds.; VCH Publishers: New York, 1988, Chapter 8.
(3) Bruice, T. C. *Acc. Chem. Res.*, **1991**, *24*, 243.
(4) Tabushi, I. *Coord. Chem. Rev.*, **1988**, *86*, 1.
(5) Traylor, T. G.; Byun, Y. S.; Traylor, P. S.; Battioni, P.; Mansuy, D. *J. Am. Chem. Soc.* **1991**, *113*, 7821.
(6) Traylor, T. G.; Isuchiya, S. *Inorg. Chem.* **1987**, *27*, 1338.
(7) Traylor, P. S.; Dolphin, D.; Traylor, T. G. *J. Chem. Soc., Chem. Commun.* **1984**, 279.
(8) Mashiko, T.; Dolphin, D.; Nakano, J.; Traylor, T. G. *J. Am. Chem. Soc.* **1985**, *107*, 3735.
(9) Traylor, T. G. *Acc. Chem. Res.* **1981**, *14*, 102.
(10) Battioni, P.; Bortok, J. F.; Mansuy, D.; Bynn, Y. S.; Traylor, T. G. *J. Chem. Soc., Chem. Commun.* **1992**, 105.
(11) Traylor, T. G.; Tsuchiya, S. *Inorg. Chem.* **1987**, *26*, 1338.
(12) Castellino, A. J.; Bruice, T. C. *J. Am. Chem. Soc.* **1988**, *110*, 158.
(13) Ostovic, D.; Bruice, T. C. *Acc. Chem. Res.* **1992**, *25*, 314.
(14) Mansuy, D. *Pure Appl. Chem.* **1987**, *59*, 759.
(15) Battioni, P.; Brigand, O.; Desvaux, H.; Mansuy, D.; Traylor, T. G. *Tetrahedron Lett.* **1991**, *32*, 2893.
(16) Artaud, I.; Grennberg, H.; Mansuy, D. *J. Chem. Soc., Chem. Commun.* **1992**, 1036.
(17) Naruta, Y.; Tani, F.; Maruyama, K. *Tetrahedron Lett.* **1992**, *83*, 1069.
(18) Mandon, D.; Oschsenbein, P.; Fischer, J.; Weiss, R.; Jayaraj, K.; Austin, R. N.; Gold, A.; White, P. S.; Brigaud, O.; Bationi, P.; Mansuy, D. *Inorg. Chem.*, **1992**, *31*, 2044.
(19) Meunier, B. *Bull. Soc. Chim. Fr. II* **1986**, *4*, 578.
(20) Hoffman, P.; Labat, G.; Robert, A. Meunier, B. *Tetrahedron Lett.* **1990**, *31*, 1991.
(21) Groves, J. T.; Haushalter, R. C.; Nakamura, M.; Nemo, T. F.; Evans, B. J. *J. Am. Chem. Soc.* **1981**, *103*, 2884.
(22) Boso, B.; Lang, A.; McMurray, T. J. *J. Chem. Phys.* **1983**, *99*, 1122.
(23) Wijesekara, T.; Matsumoto, A.; Dolphin, D.; Lexa, D. *Angew. Chem. Int. Ed. Engl.* **1990**, *102*, 1073.
(24) Tsuchiya, S.; Seno, M. *Chem. Lett.* **1989**, 263.
(25) Carrier, M. N.; Scheer, C.; Gouvine, P.; Bartoli, J. F.; Battioni, P.; Mansuy, C. *Tetrahedron Lett.* **1990**, *31*, 6645.
(26) Ellis, P. E.; Lyons, J. E. *Coor. Chem. Rev.* **1990**, *105*, 181.
(27) Bartoli, J. F.; Brigand, O.; Battioni, P.; Mansuy, D. *J. Chem. Soc., Chem. Commun.* **1991**, 440.
(28) Kadish, K. M. *Prog. Inorg. Chem.* **1986**, *34*, 435.

0020-1669/93/1332-4042$04.00/0

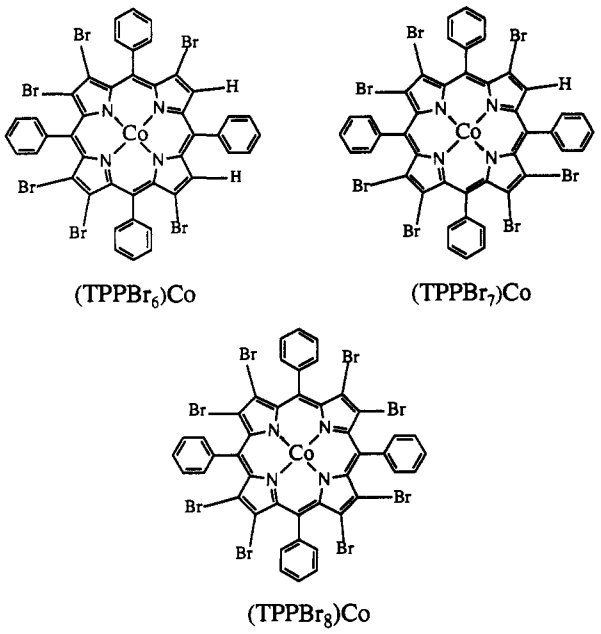

Figure 1. Structures of investigated cobalt bromoporphyrins.

Altogether, up to eight Br substituents may be added to the porphyrin periphery[10,15,18,31] and octabromo-substituted tetraphenylporphyrins of the type $(TPPBr_8)M$ where M = Fe(III), Co(II), Ni(II), Cu(II), Zn(II), and Pd(II) have been synthesized and characterized.[12-31] Complexes of $(TPPBr_x)M$ where x = 1–4 are also known,[30] but neither $(TPPBr_6)Co$ nor $(TPPBr_7)Co$ have yet been reported in the literature. Both of these derivatives are now examined in the present manuscript which describes the electrochemistry and spectroelectrochemistry of cobalt(II) tetraphenylporphyrins containing six, seven, and eight bromine atoms on the β-pyrrole positions of the porphyrin macrocycle. The structures of the investigated porphyrins are shown in Figure 1.

Experimental Section

Chemicals. Benzonitrile (PhCN) was obtained from Aldrich Chemicals and distilled over P_2O_5 under vacuum prior to use. Dimethylformamide (DMF) was purchased from J. T. Baker and distilled twice under vacuum over 4-Å molecular sieves prior to use. Tetra-*n*-butylammonium perchlorate (TBAP) was purchased from Sigma Chemicals Co., recrystallized from ethyl alcohol, and dried in a vacuum oven at 40 °C for at least 1 week prior to use. $(TPP)H_2$, (TPP)Zn, (TPP)Cu, and (TPP)Co were obtained from Strem Chemical Co. or synthesized according to literature procedures.[32]

$(TPPBr_6)H_2$ and $(TPPBr_7)H_2$. A 1.42-g sample of *N*-bromosuccinamide (NBS) (8 mM) was added to 677 mg of (TPP)Zn (1 mM) in 500 mL of CCl_4, and the reaction mixture was refluxed in the air for 4 h while being protected from moisture with a $CaCl_2$ valve. The solution was then evaporated and the residue chromatographed on neutral alumina (Merck 70–230 mesh), eluting with a 1:1 mixture of $CHCl_3$/*n*-hexane. The green fraction, which contained a mixture of $(TPPBr_6)Zn$ and $(TPPBr_7)Zn$, was collected and evaporated after which the residue was redissolved in 200 mL of CH_2Cl_2. The brominated zinc porphyrins were demetallated by adding CF_3COOH (5 mL) under nitrogen over a period of 4 h. The reaction mixture was washed, first with saturated $NaHCO_3$ and then with saturated NaCl, after which it was dried over anhydrous Na_2SO_4. The porphyrin material was then precipitated by addition of *n*-hexane (total yield 40%). After filtration, the reaction mixture was separated on a silica gel column (Merck 80–200 mesh), eluting with a 40:60 mixture of $CHCl_3$/*n*-hexane. The first fraction contained $(TPPBr_6)H_2$ and had a molecular ion peak at 1087.0 in the FAB mass spectrum (calcd 1087.1). UV–visible in benzonitrile, λ_{max}, nm ($\epsilon \times 10^4$): 454 (22.2), 553 (0.76), 594 (0.82), 725 (0.72). The second fraction obtained on elution with the solvent mixture contained $(TPPBr_7)H_2$. The molecular ion peak of this compound in the FAB mass spectrum was located at 1167.8 (calcd 1166.9). UV–visible in benzonitrile, λ_{max}, nm ($\epsilon \times 10^4$): 462 (19.1), 558 (0.67), 612 (0.64), 726 (0.67).

$(TPPBr_6)Co$ and $(TPPBr_7)Co$. About 100 mg of $(TPPBr_6)H_2$ or $(TPPBr_7)H_2$ were dissolved in 50 mL of DMF containing 200 mg of $Co(CH_3COO)_2 \cdot 2H_2O$. The solution was refluxed for 4 h and evaporated to dryness and the residue redissolved in $CHCl_3$. This solution was washed with water, dried over anhydrous Na_2SO_4 and evaporated under vacuum. The residue was chromatographed on neutral alumina using chloroform, and the first eluting band was collected, evaporated, and recrystallized from CH_2Cl_2/MeOH (yield 90%). The FAB mass spectra showed a molecular peak at 1145.1 for $(TPPBr_6)Co$ (calcd 1145.0) and 1225.2 for $(TPPBr_7)Co$ (calcd 1223.9). Anal. Calcd for $(TPPBr_6)Co$ ($C_{44}H_{22}N_4Br_6Co$): C, 46.16; H, 1.94; N, 4.60; Br, 41.87. Found: C, 46.33; H, 2.04; N, 4.70; Br, 41.60. Calcd for $(TPPBr_7)Co$ ($C_{44}H_{21}N_4Br_7Co$): C, 43.13; H, 1.73; N, 4.58; Br, 45.70. Found: C, 43.30; H, 1.87; N, 4.79; Br, 45.58.

$(TPPBr_8)H_2$ and $(TPPBr_8)Co$ were synthesized according to literature methods.[31] This involved a direct bromination of (TPP)Cu using liquid bromine in CCl_4, followed by demetallation of the resulting $(TPPBr_8)Cu$ in perchloric acid. The FAB-mass spectrum of $(TPPBr_8)H_2$ showed a molecular ion peak at 1246.0 (calcd 1245.9). Anal. Calcd for $C_{44}H_{22}N_4Br_8$: C, 42.42; H, 1.78; N, 4.49; Br, 51.30. Found: C, 42.30; H, 1.88; N, 4.41; Br, 51.18. UV–visible in benzonitrile, λ_{max}, nm ($\epsilon \times 10^4$): 471 (7.05), 570 (0.13), 638 (0.33) 745 (0.26). Cobalt insertion into $(TPPBr_8)H_2$ was carried out using the above described procedure for $(TPPBr_6)Co$ and $(TPPBr_7)Co$. Alternatively, the reaction between (TPP)Co and NBS in a $CCl_4/C_2H_4Cl_2$ mixture (1:1) at room temperature also resulted in formation of $(TPPBr_8)Co$. The molecular ion peak in the FAB mass spectrum was located at 1304.0 (calcd 1302.8). Anal. Calcd for $C_{44}H_{20}N_4Br_8Co$: C, 40.56; H, 1.55; N, 4.30; Br, 49.07. Found: C, 40.42; H, 1.54; N, 4.21; Br, 50.01. Attempts to obtain $(TPPBr_8)H_2$ using the NBS method[6-11] were unsuccessful and invariably resulted in a mixture of lower brominated products.

Instrumentation and Methods. Cyclic voltammograms were obtained with an IBM Model EC 225 voltammetric analyzer and an Ominigraphic 200 X-Y recorder using a three-electrode system. A platinum button or glassy carbon electrode was used as the working electrode. A platinum wire served as the counter electrode and a homemade saturated calomel electrode (SCE) was used as the reference electrode, which was separated from the bulk solution by a glassy diaphragm connected to a bridge filled with the supporting electrolyte. All potentials were measured vs. SCE. Unless otherwise specified, all measurements were carried out at 22 ± 1 °C. Rotating ring disk electrode experiments were performed with a MSR speed control unit (Pine Instruments Co., Grove City, NY). A platinum ring disk working electrode was utilized. Thin-layer spectroelectrochemical measurements were taken with a Tracor Northern 6500 multichannel analyzer/controller using an optically transparent platinum working electrode. UV–visible spectra of the neutral complexes were recorded using an IBM 9430 spectrophotometer. Mass spectra were obtained from a high-resolution hybrid tandem VG Analytical Model 70-SEQ and VG-4 mass spectrometers. A standard fast atom bombardment (FAB) source was used, and *m*-nitrobenzyl alcohol (NBA) was the liquid matrix. Elemental analyses were carried out by Texas Analytical Laboratories, Ind., Houston, TX.

Results and Discussion

The electrochemistry of synthetic cobalt porphyrins has been extensively studied in nonaqueous media.[28,33-42] Most Co(II)

(29) Giraudeau, A.; Callot, H. J.; Jordan, J.; Ezaher, I.; Gross, M. *J. Am. Chem. Soc.* **1979**, *101*, 3857.
(30) Giraudeau, A.; Callot, H. J.; Gross, M. *Inorg. Chem.* **1979**, *18*, 201.
(31) Byrappa, P.; Krishnan, V. *Inorg. Chem.* **1991**, *36*, 239.
(32) Fuhrhop, J.-H.; Smith, K. M. In *Porphyrins and Metalloporphyrins*; Smith, K. M., Ed.; Elsevier: New York, 1975; Chapter 19.
(33) Fuhrhop, J. H.; Kadish, K. M.; Davis, D. G. *J. Am. Chem. Soc.* **1973**, *95*, 5164.
(34) Kadish, K. M.; Bottomley, L. A.; Beroiz, D. *Inorg. Chem.* **1978**, *17*, 1124.
(35) Kadish, K. M.; Lin, X. Q.; Han, B. C. *Inorg. Chem.* **1987**, *26*, 4161.
(36) Maiya, G. B.; Han, B. C.; Kadish, K. M. *Langmuir* **1989**, *5*, 645.
(37) Mu, X. H.; Lin, X. Q.; Kadish, K. M. *Electroanalysis* **1989**, *1*, 113.
(38) Lin, X. Q.; Boisselier-Cocolios, B.; Kadish, K. M. *Inorg. Chem.* **1986**, *25*, 3242.
(39) Kadish, K. M.; Araullo-McAdams, C.; Han, B. C.; Frazen, M. M. *J. Am. Chem. Soc.* **1990**, *112*, 8364.
(40) Truxillo, L. A.; Davis, D. G. *Anal. Chem.* **1975**, *47*, 2260.
(41) Felton, R. H.; Linschitz, H. *J. Am. Chem. Soc.* **1966**, *88*, 1113.

derivatives undergo three one-electron oxidations, the first of which generates either a Co(II) π cation radical or a Co(III) species depending upon solution conditions. At least one and possibly two one-electron reductions can also be observed for most compounds. The first corresponds to the formation of a cobalt(I) complex while the second involves the generation of a cobalt(I) porphyrin π anion radical. Only two monomeric cobalt complexes are known to deviate substantially from this type of behavior. These are $[(CN)_4TPP]Co$ and $[(TMPyP)Co^{II}]^{4+}$, both of which have electron-withdrawing substituents on the porphyrin macrocycle.[38,39] $[(TMPyP)Co^{II}]^{4+}$ is reduced by a total of six electrons in four steps[39] while $[(CN)_4TPP]Co$ undergoes three one-electron reductions, the first of which generates a Co(II) π anion radical followed by formation of a Co(I) porphyrin π anion radical and dianion.[38]

The $(TPPBr_x)Co$ complexes investigated in the present study all undergo three one-electron oxidations, a single reversible one-electron reduction and an irreversible multielectron reduction at more negative potentials. As will be demonstrated, the first one-electron oxidation involves formation of $[(TPPBr_x)Co^{III}]^+$ while the first one-electron reduction generates $[(TPPBr_x)Co^{I}]^-$. The UV–visible spectra of each singly-oxidized and singly-reduced species as well as the redox potentials for their formation were examined as a function of the number of Br substituents and an overall mechanism for the multielectron reduction is presented.

Electrooxidation of $(TPPBr_x)Co$, Where $x = 6$, 7, or 8. Figure 2 illustrates cyclic voltammograms for the oxidation of (TPP)Co and $(TPPBr_x)Co$ in PhCN containing 0.1 M TBAP. The first oxidation of (TPP)Co has been characterized by cyclic voltammetry in a variety of noncoordinating solvents[28] and involves noncoupled oxidation/reduction processes which, in PhCN, occur at $E_{pa} = 0.62$ and $E_{pc} = 0.38$ V for a scan rate of 0.1 V/s. The second and third oxidations of (TPP)Co are both reversible and occur at $E_{1/2} = 1.20$ and 1.39 V.

Three one-electron oxidations are also observed for $(TPPBr_x)Co$, with both the reversibility of the first process and the separation between the latter two depending upon the number of Br groups of $TPPBr_x$. For example, the Co(II)/Co(III) process of (TPP)Co is characterized by an $|E_{pa} - E_{pc}|$ of 240 mV and this separation may be compared to peak separations of 200 mV for the first oxidation of $(TPPBr_6)Co$, 120 mV for $(TPPBr_7)Co$, and 60 mV for $(TPPBr_8)Co$ under the same experimental conditions. In addition, the second and third oxidations of $(TPPBr_x)Co$ are overlapped in potential and this is not the case for (TPP)Co which shows two well-separated one-electron transfer reactions corresponding to the stepwise formation of a Co(III) π cation radical and dication. All three brominated cobalt(II) porphyrins also show an additional rereduction process at $E_{pc} \sim 0.92$ V. This peak is not present if the positive potential scan is terminated at + 1.2 V and only appears when the potential is scanned to sufficiently positive values for electrogeneration of $[(TPPBr_x)Co^{III}]^{3+}$. Its origin is unclear but its potential is invariant with changes in the number of Br substituents on the porphyrin macrocycle.

The first oxidation of cobalt(II) porphyrins can occur at either the metal center or at the conjugated macrocycle,[28] and a differentiation of these two processes can be easily made on the basis of IR[44,47,48] or UV–visible spectroscopy.[37,43–48] A Co(III) derivative is formed upon oxidization of (TPP)Co in PhCN,[28] and this is also the case upon the abstraction of one-electron from $(TPPBr_x)Co$. Similar UV–visible spectra are seen for each singly oxidized species and an example of the spectral changes which occur during the first controlled-potential oxidation of $(TPPBr_8)Co$ is shown in Figure 3a. The spectral changes are reversible and the final UV–visible spectrum is typical of a cobalt(III) porphyrin of the type $[(P)Co^{III}]^+$.[37,43]

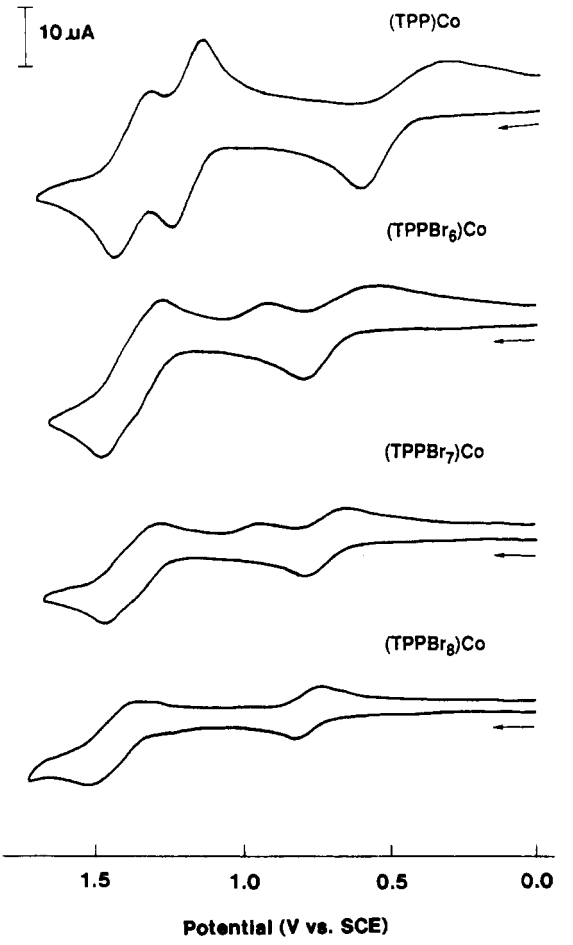

Figure 2. Cyclic voltammograms of $(TPPBr_x)Co$ in PhCN containing 0.1 M TBAP.

A comparison of the UV–visible spectra for each $[(TPPBr_x)Co^{III}]^+$ and $(TPPBr_x)Co^{II}$ derivative is given in Figure 4, and the spectral data are summarized in Table II. Each Co(III) and Co(II) complex is characterized by a single Soret band, the former of which is red shifted with respect to the latter. The Co(III) porphyrin has two visible bands, both of which are red shifted with respect to the single visible band of the corresponding Co(II) derivative. The highest values of molar absorptivities are obtained for $(TPP)Co^{II}$ and $[(TPP)Co^{III}]^+$ while the lowest are seen for $(TPPBr_8)Co^{II}$ and $[(TPPBr_8)Co^{III}]^+$. Intermediate values of ϵ are seen for the two $TPPBr_6$ and $TPPBr_7$ derivatives in each oxidation state.

The porphyrin absorption bands undergo a progressive red shift with increase in the number of the Br groups on $TPPBr_x$, and the overall magnitude of the shift ranges from 36 to 39 nm between the Soret band of TPP and that of $TPPBr_8$, independent of the metal ion oxidation state. In addition, each band becomes broader with increase in number of Br groups on the macrocycle. A similar observation has been reported for β-substituted porphyrins with other central metal ions and this was interpreted in terms of configurational interactions.[31]

Electroreduction. Figure 5 depicts the electroreduction of $(TPPBr_x)Co$ by cyclic voltammetry in PhCN containing 0.1 M TBAP. The first reduction is reversible for all four porphyrins

(42) Lexa, D.; Saveant, J. M.; Soufflet, J. P. *J. Electroanal. Chem.* **1979**, *100*, 159.
(43) Araullo-McAdams, C.; Kadish, K. M. *Inorg. Chem.* **1990**, *29*, 2749.
(44) Hu, Y.; Han, B. C.; Bao, L. Y.; Mu, X. H.; Kadish, K. M. *Inorg. Chem.* **1991**, *30*, 2444.
(45) Mu, X. H.; Kadish, K. M. *Inorg. Chem.* **1989**, *28*, 3743.
(46) Scholz, W. F.; Reed, C. A.; Lee, Y. J.; Scheidt, W. R.; Lang, G. J. *J. Am. Chem. Soc.* **1982**, *104*, 6791.
(47) Hinman, A. S.; Pavelich, B. J.; McGarty, K. *Can. J. Chem.* **1988**, *66*, 1589.
(48) Jones, D. H.; Hinman, A. S. *J. Chem. Soc., Dalton Trans* **1992**, 1503.

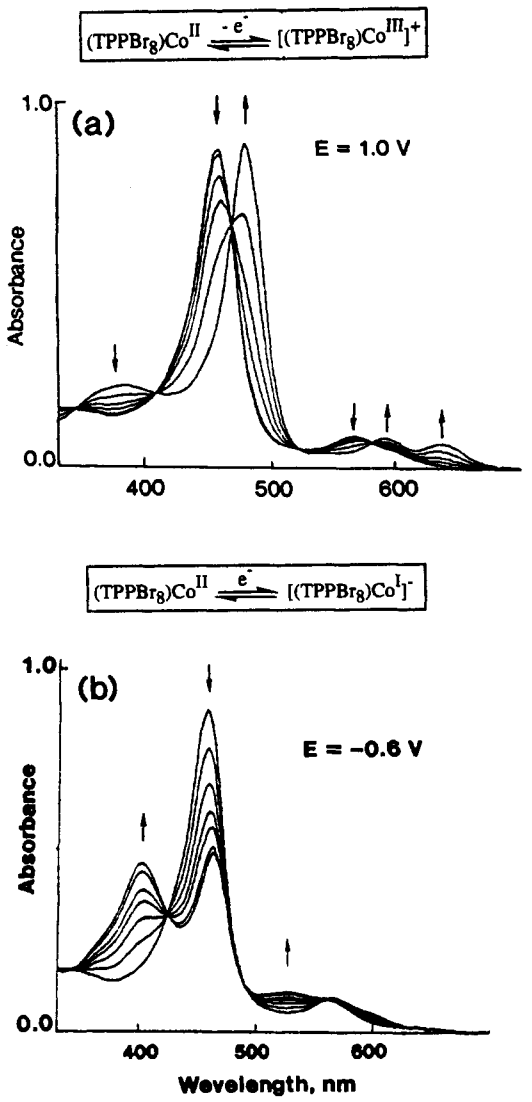

Figure 3. Thin layer spectral changes obtained upon (a) the first one-electron oxidation and (b) the first one-electron reduction of $(TPPBr_8)$-Co in PhCN containing 0.1 M TBAP.

Table I. Half-Wave Potentials (V vs SCE) for the Electrode Reactions of $(TPPBr_x)Co$ in Benzonitrile Containing 0.1 M TBAP

	oxidation			reduction	
compound	3rd	2nd	1st	1st	2nd
(TPP)Co	1.39	1.20	0.52[a]	-0.85	-1.97
$(TPPBr_6)Co$	1.46	1.31	0.80[a]	-0.45	
$(TPPBr_7)Co$	1.43	1.31	0.78[a]	-0.41	
$(TPPBr_8)Co$	1.40	1.33	0.75	-0.35	

[a] Peak potential, E_{pa}, at 0.1 V/s.

and a $[(P)Co^I]^-$ complex is generated at potentials between $E_{1/2}$ = -0.85 V (P = TPP) and -0.35 V (P = $(TPPBr_8)$. This 500-mV difference between the Co(II)/Co(I) processes of the two complexes may be compared to an approximate separation of 240 mV between the first one-electron oxidations of the same two porphyrins to generate a Co(III) derivative. The values of $E_{1/2}$ for reduction are linearly related to the number of Br groups on the macrocycle and the resulting slope of $\Delta E_{1/2}/\Delta Br = 63$ mV can be compared to 70 and 135 mV slopes obtained from similar plots for the first two one-electron reductions of $(TPPBr_x)H_2$ in CH_2Cl_2 where $x = 1$–4.[29]

The reversible $E_{1/2}$ for reduction of $[(TPP)Co^I]^-$ is located at -1.97 V in PhCN while $[(TPPBr_x)Co^I]^-$ begins to be reduced at potentials greater than -1.4 V. The currents for these latter reductions are substantially higher than those for the first one-electron reduction of the same compound, and this suggests either the occurrence of a catalytic process or a multielectron transfer. As will be demonstrated, the latter is the case with the mechanism involving a stepwise reductive elimination of Br^- to generate $[(TPP)Co]^-$ as the final porphyrin product in solution. Initial suggestions for this mechanism come from cyclic voltammograms of the type shown in Figure 5. A new redox couple is seen on the anodic potential sweep after scanning past the multielectron reduction and the potential of this couple (-0.85 V) matches exactly the $E_{1/2}$ for oxidation of singly-reduced $[(TPP)Co^I]^-$. The formation of $[(TPP)Co]^-$ is unexpected and can only be accounted for a complete loss of all the Br groups during electroreduction of $[(TPPBr_x)Co]^-$. Evidence for the formation of Br^- is given by experiments carried out at a rotating ring disk electrode while additional proof for $[(TPP)Co]^-$ generation is obtained by thin-layer spectroelectrochemistry.

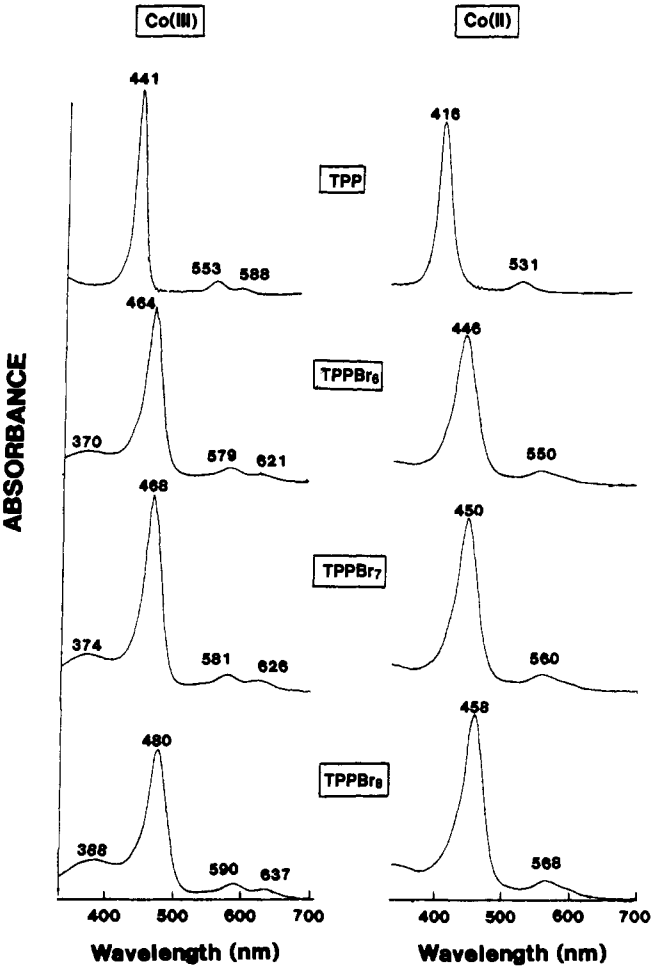

Figure 4. UV–visible spectra of neutral and singly oxidized $(TPPBr_x)Co$ in PhCN containing 0.1 M TBAP.

Table II. UV–Visible Spectral Data for Co(I), Co(II), and Co(III) Derivatives of $TPPBr_x$ in PhCN Containing 0.1 M TBAP

metal ion	porphyrin macrocycle	abs bands λ, nm (ε × 10⁻⁴)			
Co(I)	TPP	364.4 (5.37)	428.1 (7.02)	513.6 (1.50)	
	$TPPBr_6$	392.3 (4.89)	452.9 (6.60)	518.4 (1.31)	
	$TPPBr_7$	395.7 (4.74)	457.1 (5.58)	520.1 (1.11)	
	$TPPBr_8$	402.2 (4.54)	463.5 (4.56)	527.2 (1.07)	
Co(II)	TPP		416.8 (17.85)	530.7 (1.26)	
	$TPPBr_6$		446.4 (13.49)	550.0 (1.23)	
	$TPPBr_7$		450.0 (12.10)	560.2 (1.16)	
	$TPPBr_8$		458.2 (8.03)	568.0 (1.03)	
Co(III)	TPP	322.8 (1.72)	440.5 (21.09)	552.6 (1.35)	587.9 (0.61)
	$TPPBr_6$	370.4 (2.23)	463.5 (13.73)	579.1 (1.00)	620.9 (0.54)
	$TPPBr_7$	373.5 (2.11)	467.7 (11.97)	581.4 (0.95)	626.2 (0.63)
	$TPPBr_8$	388.1 (2.19)	480.0 (8.16)	589.7 (0.86)	636.9 (0.59)

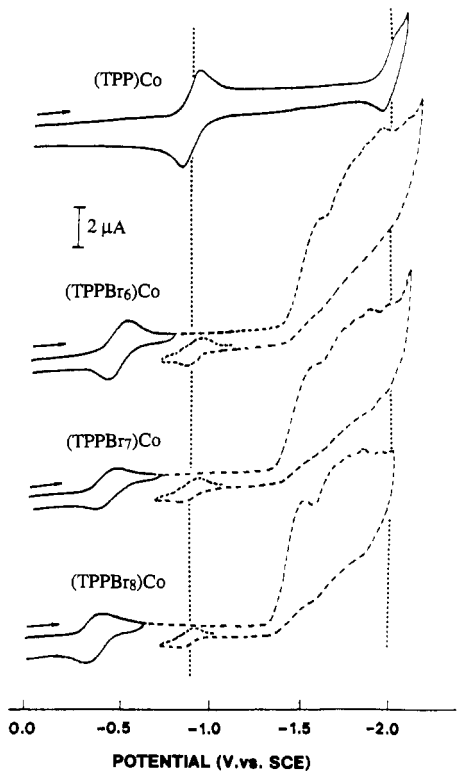

Figure 5. Cyclic voltammograms for the first (–) and following (- - -) reductions of $(TPPBr_x)Co$ in PhCN containing 0.1 M TBAP.

The data for reduction of $(TPPBr_8)Co$ at a rotating ring disk electrode in DMF are shown in Figure 6. The disk potential was scanned in a cathodic direction from 0.0 to –2.0 V while the ring potential was held at either 0.00 or 0.90 V in order to observe a reoxidation of the electroactive species generated at the disk. The first reduction of $(TPPBr_8)Co$ occurs at $E_{1/2} = -0.35$ V as measured by cyclic voltammetry and a similar value of $E_{1/2}$ is calculated from the current voltage curve in Figure 6. The second reduction of $(TPPBr_8)Co$ begins to occur at ≈ -1.35 V and the current for this process is approximately 8 times higher than that for the first reduction. Two oxidation processes are observed when the ring potential is held at 0.0 V. The first occurs at $E_{1/2} = -0.35$ V and corresponds to the simple reoxidation of electroreduced $[(TPPBr_8)Co^I]^-$. The second oxidation of electroreduced $(TPPBr_8)Co$ occurs at approximately –1.35 V and has currents much smaller than that of the first one-electron reoxidation. This reaction can be associated with reoxidation of the electrogenerated cobalt(I) π anion radical but, as discussed in the following sections, this species undergoes a rapid chemical reaction prior to reoxidation, thus resulting in a substantially lower current at the disk. Two processes also occur at the disk when the potential of the ring is held to 0.90 V (Figure 6b). The first is similar to what is observed when the disk is held at 0.00 V (Figure 6a) and is assigned as a simple reoxidation of electrogenerated $[(TPPBr_8)Co^I]^-$ while the second is much larger in current and is assigned in large part to an oxidation of liberated Br^- in solution.[49]

As seen in Figure 5 the electroreductive debromination of $[(TPPBr_x)Co]^-$ begins to occur at potentials negative of –1.40 V for $x = 8$ or negative of –1.50 V for $x = 6$. These results suggest that Br^- loss occurs immediately after formation of a porphyrin π anion radical which should be generated at approximately these potantials.[28] The loss of Br^- must also be accompanied by hydrogen abstraction from the solvent and the overall mechanism is therefore proposed to occur as shown in Scheme I.

(49) The oxidation of Br^- in DMF containing 0.1 M tetra-*n*-butylammonium bromide occurs at $E_{pa} \approx 0.90$ V.

The rate for conversion of $[(TPPBr_x)Co^I]^{2-\bullet}$ to $[TPPCo^I]^-$ can be slowed down at low temperature, and this is illustrated by variable temperature cyclic voltammograms for the electroreduction of $(TPPBr_7)Co$ in DMF. Three one-electron reductions are seen at –60 °C. The first two are quasireversible and occur at $E_{1/2} = -0.42$ and –1.38 V. The third is irreversible and is located at $E_{pa} = -1.90$ V for a scan rate of 0.1 V/s. This latter reaction most likely corresponds to formation of a cobalt(I) porphyrin dianion.

The most definitive evidence for the stepwise loss of Br^- and the ultimate formation of $[(TPP)Co^I]^-$ comes from a comparison of UV–visible spectra for genuine cobalt(I) porphyrins and those obtained during controlled reduction of $[(TPPBr_x)Co^I]^-$ at various potentials along the multielectron reduction wave. An example of the spectral changes obtained upon conversion of $(TPPBr_8)Co$ to $[(TPPBr_8)Co^I]^-$ is shown in Figure 3b. As the reduction proceeds, all bands of the initial species decrease in intensity as new bands grow in at 403, 462, and 516 nm. The spectrum after complete electrolysis shows a split Soret band and two blue-shifted visible bands, both of which are consistent with formation of $[(TPPBr_8)Co^I]^-$.[44] These spectral changes are reversible, and stepping the potential back to 0.0 V regenerates the UV–visible spectrum of the initial Co(II) complex.

Similar spectral changes are obtained during reduction of the other two brominated porphyrins and all four Co(I) spectra are illustrated in Figure 7a. The key point in this figure is that the wavelengths and ratio of molar absorptivities are unique for each cobalt(I) porphyrin and these data can therefore be utilized to spectrally monitor the loss of Br^- upon controlled potential reduction of $[(TPPBr_8)Co]^-$. Scheme I predicts the formation of lower brominated porphyrins prior to the ultimate generation of $[(TPP)Co^I]^-$, and up to seven different $[(TPPBr_x)Co^I]^-$ species might therefore be generated as transients, each of which would have a different reduction potential whose $E_{1/2}$ would become more negative with decrease in the number of Br substituents on the macrocycle. This should be reflected by a series of irreversible reduction peaks in the cyclic voltammograms, and this is indeed the case as seen in Figure 5.

The formation of lower brominated $[(TPPBr_x)Co^I]^-$ complexes is also be seen by spectrally monitoring the reduction of $[(TPPBr_x)Co^I]^-$ as a function of applied potential. These data are shown in Figure 7b. The spectral changes are irreversible, and no isosbestic points are observed. The final spectra are similar to those shown in Figure 7a, and on the basis of these data, the porphyrins generated at –1.56 and –1.70 V can be assigned to partially brominated Co(I) complexes. The relative ratios of the split Soret band intensities as well as the absolute position of the peak maxima correspond to the formation of $[(TPPBr_3)Co^I]^-$ after reduction at –1.56 V and to $[(TPPBr_1)Co^I]^-$ after reduction at –1.70 V. The spectrum at –1.80 V is identical with that of genuine $[(TPP)Co^I]^-$, and this agrees with the mechanism proposed in Scheme I.

Finally it should be pointed out that the difference between spectra of genuine $[(TPP)Co^I]^-$ and $[(TPPBr_x)Co^I]^-$ parallel spectral differences between $(TPP)Co$ and $(TPPBr_8)Co$ or $[(TPP)Co^{III}]^+$ and $[(TPPBr_8)Co^{III}]^+$. The split Soret band of $[(TPPBr_x)Co^I]^-$ shifts from 364 and 428 to 402 and 463 nm upon going from TPP to $TPPBr_8$ and this 35–38-nm difference in λ_{max} can be compared to an overall 37–39-nm difference in λ_{max} for the Soret bands of the neutral and singly oxidized forms of the same two porphyrins. The Soret and visible bands also broaden with increase in the number of Br groups and the lowest values of ϵ are obtained for $[(TPPBr_8)Co^I]^-$ (see Figure 7a and Table II).

Correlations between the Soret band energy and the number of Br substituents on $[(TPPBr_x)Co^I]^-$, $(TPPBr_x)Co^{II}$, and $[(TPPBr_x)Co^{III}]^+$ are all linear (Figure 8a), and this demonstrates that the electronic effect induced by the substituents

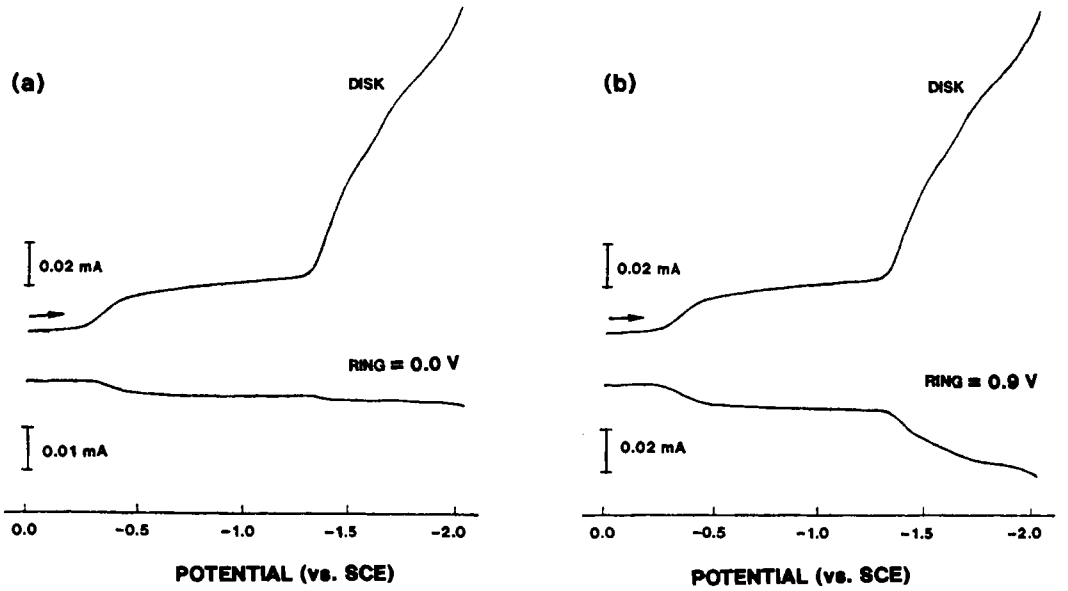

Figure 6. Rotating ring disk voltammogram of $(TPPBr_8)Co$ in DMF containing 0.1 M TBAP for ring potentials of (a) 0.00 and (b) 0.90 V vs SCE.

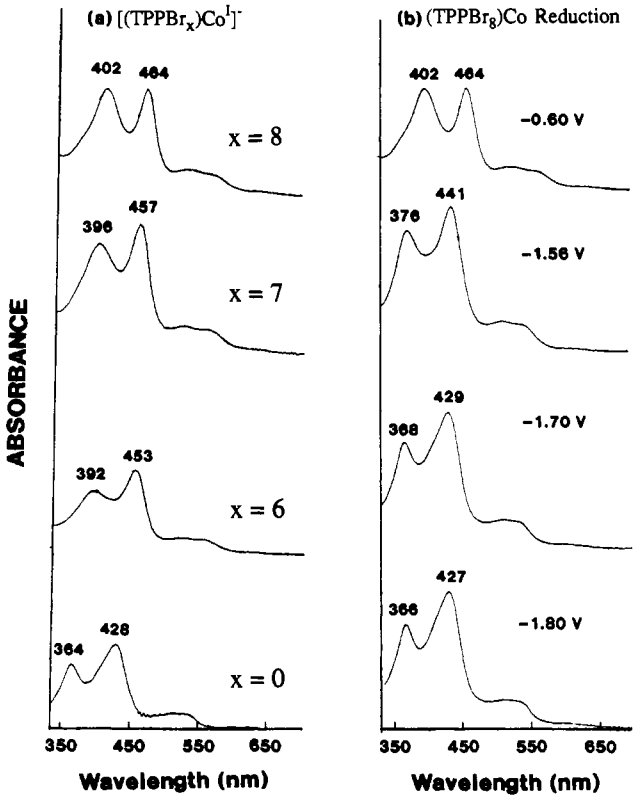

Figure 7. UV–visible spectra of (a) $[(TPPBr_x)Co^I]^-$ where $x = 8$, 7, 6, or 0 and (b) the product of $(TPPBr_8)Co$ reduction as a function of applied potential.

Scheme I

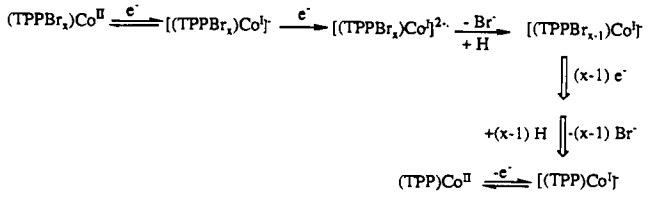

varies linearly with the transition energy of the investigated cobalt porphyrin. The magnitude of the substituent effect depends upon the oxidation state of the central metal ion and follows the order Co(II) > Co(III) > Co(I). As earlier discussed, a linear

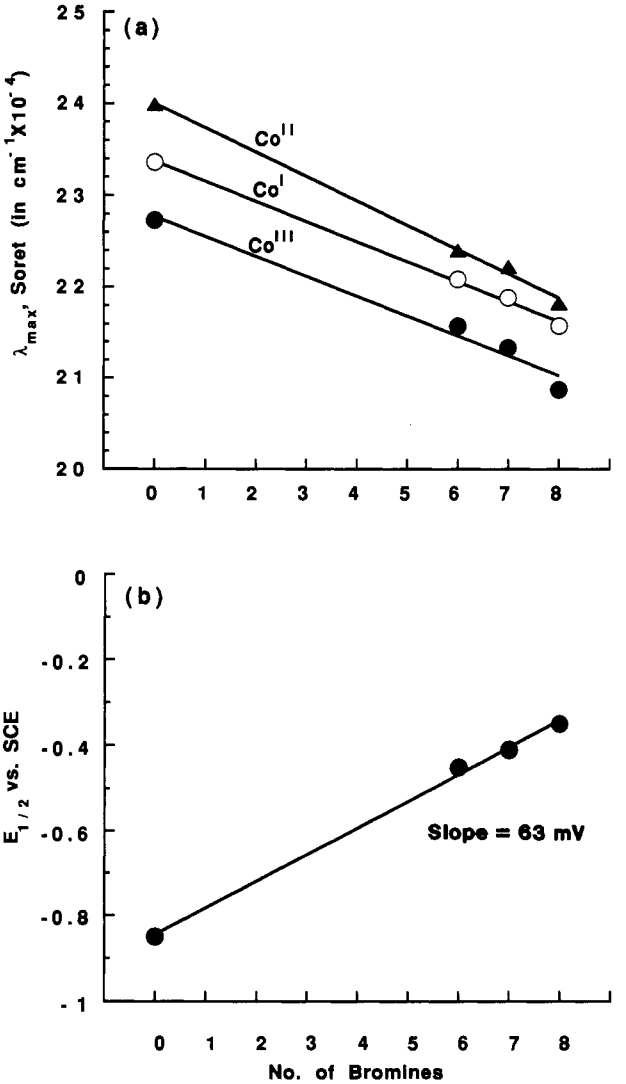

Figure 8. Dependence of (a) Soret band position of Co(I), Co(II), and Co(III) derivatives and (b) reversible Co(II) reduction potential on the number of Br substituents of the $(TPP)Br_x$ macrocycle.

relationship is also seen between the number of Br groups on $(TPPBr_x)Co$ and $E_{1/2}$ for the Co(II)/Co(I) process of these compounds. This plot is shown in Figure 8b, and the slope of 63

mV can be compared to an approximate $\Delta E_{1/2}/\Delta Br$ of ~30 mV for the Co(II)/Co(III) reaction of the same series of compounds. However, a quantitative measurement cannot be made for the electrooxidation due to the irreversibility of this reaction for (TPP)Co and the lower brominated complexes in the (TPP-Br_x)Co series.

In summary, cobalt tetraphenylporphyrins bearing six, seven, or eight Br substituents on the β-pyrrole positions undergo three-one-electron oxidations and up to nine one-electron reductions. The first oxidation involves the reversible formation of $[(TPPBr_x)Co^{III}]^+$ while the first reduction involves the reversible formation of $[(TPPBr_x)Co^{I}]^-$. As expected, both reactions occur at potentials which are cathodically shifted from $E_{1/2}$ for the oxidation or reduction of (TPP)Co under the same experimental conditions. Electrogenerated $[(TPPBr_x)Co^{III}]^+$ and $[(TPPBr_x)Co^{I}]^-$ are both stable on the cycle voltammetric and spectroelectrochemical time scales, but a chemical reaction occurs immediately after the apparent formation of a cobalt(I) π anion radical and results in the ultimate generation of $[(TPP)Co]^-$, which is detected both electrochemically and spectrally. This reaction proceeds via a series of lower brominated derivatives, each of which has a reduction potential which becomes more negative as the number of Br groups on $TPPBr_x$ is decreased.

Finally it should be pointed out that the 500 mV difference in potential between $E_{1/2}$ for reduction of $[(TPPBr_8)Co^{I}]^-$ and $E_{1/2}$ for reduction of $[(TPP)Co^{I}]^-$ suggests that porphyrins containing a given number of Br substituents between 1 and 7 might be quantitatively electrosynthesized by electroreduction of $[(TPPBr_8)Co^{I}]^-$ at a predetermined constant controlled potential. Experiments along these lines are now in progress.

Acknowledgment. The support of the National Science Foundation (Grant No. CHE 8822881) and the National Institutes of Health (GM 25172) and an LGIA grant from the University of Houston is gratefully acknowledged. The authors also acknowledge Dr. Giuseppe D'Arcangelo of Il Universitá degli Studi di Roma for the mass spectral measurements.